ABCA3 inactivation in mice causes respiratory failure, loss of pulmonary surfactant, and depletion of lung phosphatidylglycerol[S]

Michael L. Fitzgerald,[*,†] Ramnik Xavier,[†] Kathleen J. Haley,[§] Ruth Welti,[**] Julie L. Goss,[*] Cari E. Brown,[*,†] Debbie Z. Zhuang,[*,†] Susan A. Bell,[*] Naifang Lu,[†] Mary Mckee,[††] Brian Seed,[†] and Mason W. Freeman[1,*,†]

Lipid Metabolism Unit,* Center for Computational and Integrative Biology,† and Program in Membrane Biology,†† Massachusetts General Hospital, Harvard Medical School, Boston, MA 02114; Division of Pulmonary and Critical Care Medicine,§ Department of Medicine, Brigham and Women's Hospital and Harvard Medical School, Boston, MA 02364; and Division of Biology,** Kansas State University, Manhattan, KS 66506

Abstract The highly branched mammalian lung relies on surfactant, a mixture of phospholipids, cholesterol, and hydrophobic proteins, to reduce intraalveolar surface tension and prevent lung collapse. Human mutations in the ABCA3 transporter have been associated with childhood respiratory disease of variable severity and onset. Here, we report the generation of *Abca3* null mice, which became lethargic and cyanotic and died within 1 h of birth. Tissue blots found ABCA3 expression was highest in lung but was also detectable in other tissues, including the kidney. Gross development of kidney and lung was normal in neonatal Abca3$^{-/-}$ pups, but the mice failed to inflate their lungs, leading to death from atelectatic respiratory failure. Ultrastructural analysis of the Abca3$^{-/-}$ lungs revealed an absence of surfactant from the alveolar space and a profound loss of mature lamellar bodies, the intracellular storage organelle for surfactant. Mass spectrometry measurement of >300 phospholipids in lung tissue taken from Abca3$^{-/-}$ mice showed a dramatic reduction of phosphatidylglycerol (PG) levels as well as selective reductions in phosphatidylcholine species containing short acyl chains. These results establish a requirement of ABCA3 for lamellar body formation and pulmonary surfactant secretion and suggest a unique and critical role for the transporter in the metabolism of pulmonary PG. They also demonstrate the utility of the Abca3 null mouse as a model for a devastating human disease.— Fitzgerald, M. L., R. Xavier, K. J. Haley, R. Welti, J. L. Goss, C. E. Brown, D. Z. Zhuang, S. A. Bell, N. Lu, M. Mckee, B. Seed, and M. W. Freeman. **ABCA3 inactivation in mice causes respiratory failure, loss of pulmonary surfactant, and depletion of lung phosphatidylglycerol. *J. Lipid Res.* 2007.** 48: **621–632.**

Supplementary key words ATP cassette binding transporter A1 • lipid transporter • lamellar body

ABC transporters are large polytopic membrane proteins that move molecules across bilayer membranes by hydrolyzing ATP. The A class of this gene family has at least 11 members and has evolved rapidly during the vertebrate radiation (1). The functional importance of the A class transporters is clear, as mutations in members of the class cause Tangier disease (ABCA1), Stargardt's macular degeneration (ABCA4), and harlequin icthyosis (ABCA12), disorders in which defects in transporter activity lead to major disruptions in human physiology (2–5). Recently, mutations in the gene encoding the ABCA3 transporter were associated with human respiratory diseases with either a neonatal or later childhood onset (6–8).

A role for ABCA3 in lung function was first indicated when antibodies against the transporter were found to stain type II alveolar cells at the plasma membrane as well as at the limiting membrane of lamellar bodies (9, 10). The lamellar body is a unique lysosome-derived storage organelle characterized by internal lamellae enriched in the phospholipids, cholesterol, and hydrophobic proteins that constitute pulmonary surfactant. Through a process of regulated exocytosis, the type II cells secrete stored pulmonary surfactant into the alveolar space, where it functions to reduce surface tension at low lung volumes and thus prevents alveolar collapse. Considering the close homology between ABCA3 and ABCA1, it is reasonable to suspect that, like ABCA1, ABCA3 may be involved in a lipid-trafficking step, possibly at the limiting membrane of

Abbreviations: apoA-I, apolipoprotein A-I; BAC, bacterial artificial chromosome; PC, phosphatidylcholine; PE, phosphatidylethanolamine; PG, phosphatidylglycerol; PI, phosphatidylinositol; PS, phosphatidylserine; SM, sphingomyelin.

[1] To whom correspondence should be addressed.
e-mail: freeman@molbio.mgh.harvard.edu

[S] The online version of this article (available at http://www.jlr.org) contains three supplemental figures, one video and one table.

Manuscript received 10 October 2006 and in revised form 28 November 2006.

Published, JLR Papers in Press, December 1, 2006.
DOI 10.1194/jlr.M600449-JLR200

the lamellar body. Indeed, Cheong et al. (11) presented data analyzing cells transfected with an ABCA3 cDNA, or with a small interfering RNA targeting the endogenous ABCA3 message, and concluded that ABCA3 can stimulate the uptake of fluorescently labeled analogs of phosphatidylcholine (PC), sphingomyelin (SM), and cholesterol, suggesting that the transporter may have broad lipid transport activity, not unlike ABCA1, but opposite in direction.

Human mutations in ABCA3 have been associated with respiratory disease of variable onset and severity, but the precise role of ABCA3 in pulmonary function is unknown. To explore the physiologic transport function of ABCA3, we engineered mice that lack ABCA3 expression. Null embryos were generated in Mendelian frequencies and had grossly normal development in utero. In contrast, at birth, despite attempts to clear their lungs of fluid and initiate breathing, the Abca3$^{-/-}$ mice rapidly became cyanotic and perished within 1 h. Histologic and ultrastructural analysis of Abca3$^{-/-}$ lung tissue indicated an invariable collapse of the airspaces at birth and a profound lack of secreted surfactant. These findings were associated with a failure to develop mature lamellar bodies in the alveolar type II cells. This phenotype was also associated with a dramatic reduction in lung phosphatidylglycerol (PG) and lesser reductions in PC species with short acyl chains, suggesting a lipid transport activity that, to date, appears unique among the members of the A class of the ABC transporter superfamily.

METHODS

Reagents

A rabbit anti-ABCA3 antibody was generated against the last 100 amino acids of mouse ABCA3, as described previously (12). To generate a mouse ABCA3 cDNA, an Open Biosystems (Huntsville, AL) clone (No. 5044171) was sequenced on both strands, confirming that it represented nucleotides 960–5,779 of the mouse cDNA and contained no mutations. However, this clone lacked nucleotides 1–954, which code for the first 167 amino acids of the open reading frame. Reverse transcription-PCR amplification of a mouse lung mRNA pool generated a 1.4 kb product containing the missing sequences that was inserted back into the cDNA as a *Kpn*I/*Afe*I restriction fragment. Sequence analysis of the resulting clone showed that it represented an intact error-free open reading frame.

Animal care

All animal procedures were approved by the Massachusetts General Hospital Subcommittee on Research Animal Care and were conducted in accordance with the U.S. Department of Agriculture Animal Welfare Act for the Humane Care and Use of Laboratory Animals.

Generation of Abca3 knockout mice

The *Abca3* locus was disrupted in mouse 129/SvEv embryonic stem cells using an *Abca3*-targeted bacterial artificial chromosome (BAC) as described previously (13). In brief, using lambda red-mediated recombination in bacteria, a BAC from a 129 genomic library containing the *Abca3* locus had exons 4 and 5 replaced with a zeo^r/neo^r dual selection cassette. Insertion of the cassette at exon 4 produces a targeted locus capable of generating only truncated ABCA3 peptides encoding the first 17 amino acids of the transporter. The structure of the targeted BAC, verified by PCR and Southern blotting, was linearized and electroporated into 129/SvEv cells. Two G418-resistant colonies screened for the lack of BAC vector sequences and showing only two fluorescent in situ hybridization signals were selected for injection into C57BL/6 blastocysts. This screening ensured that the injected clones had no illegitimate copies of the BAC and that the targeted *Abca3* allele had replaced one of the wild-type *Abca3* alleles. Two chimeric lines were produced, one of which transmitted the targeted allele to F1 progeny as analyzed by multiplex PCRs (P1, 5′-TCCTCTAAGGGCATGTTCAGG-3′; P2, 5′-ATGGCCACCCT-TCCTTGGGTC-3′; P3, 5′-GGCCAGGGTGTTGTCCGGCACC-3′) and Southern blotting of genomic *Bam*HI digests with a probe against nucleotides 8,555–9,075 located in the third intron of the *Abca3* locus.

ABCA3 tissue and macrophage immunoblots

The specificity of the anti-ABCA3 antibody was tested using cell lysates from 293-EBNA-T cells transfected with empty vector or with cDNAs for ABCA1, ABCA2, ABCA7, and ABCA3 (20 μg of total cell protein in a lysis buffer composed of 20 mM Tris-HCl, pH 7.5, 150 mm NaCl, 1 mM EDTA, 1% Nonidet P-40, 0.5% deoxycholate, 0.1% SDS, and 0.001% Sigma protease cocktail). The lysates were separated by 6% SDS-PAGE and transferred to nitrocellulose. Membranes were blocked overnight at 4°C in blocking buffer (1% BSA, 5% dried milk protein, and 0.1% Tween-20 in 1× PBS) and then incubated with either preimmune or immune serum at a 1:1,000 dilution. Antibody binding was detected with a horseradish peroxidase-conjugated goat anti-rabbit IgG antibody, enhanced chemiluminescence (Pierce), and X-ray film. Only the immune serum detected two bands of ~180 and 150 kDa in the lysates from the ABCA3 transfected cells (**Fig. 1C**). The 150 kDa isoform comigrated with the most prominent isoform detected in lung. The expression of ABCA3 protein in tissues from wild-type adult C57BL/6 mice was assessed in lysates (50 μg of total cell protein) prepared and analyzed as described above (Fig. 1C). For the analysis of ABCA3 protein in tissues of Abca3$^{+/-}$ mice, either 15 or 20 μg of total cell protein was used as indicated (Fig. 1E). Bone marrow macrophages were isolated by flushing femurs of C57BL/6 mice with cold DMEM and collecting the marrow by spinning at 2,200 rpm. Red blood cells were lysed with 0.17 M NH_4Cl, and bone marrow was suspended in DMEM supplemented with 10% fetal bovine serum, 100 U/ml penicillin, 100 μg/ml streptomycin, and 15% L929-conditioned medium. After 24 h of culture, the nonadherant cells were collected and cultured for an additional 6 days to obtain mature macrophages.

To obtain alveolar macrophages, bronchial alveolar lavage was performed on adult mice by inserting a 22G Abbocath-T catheter (Abbot) into the trachea of euthanized mice and flushing the lungs with five 1 ml aliquots of Hank's balanced salt solution. The combined aliquots were spun at 250 *g* for 5 min to pellet the alveolar macrophages. The cell pellet was washed once with 1× PBS and lysed in lysis buffer as described above.

Histological analysis

Lung architecture was assessed in E18.5 embryos that had not respired, or in postnatal day 0 pups that had respired, as described previously (14). To assess airspace morphometry, the mean chord length of the saccule airspaces in five randomly chosen microscopic fields of each sample was measured by a blinded viewer using a Leica DMLB microscope interfaced with Leica Q Win 550 image-analysis software (Leica Microsystems, Inc.). The development of the pulmonary airways and vascula-

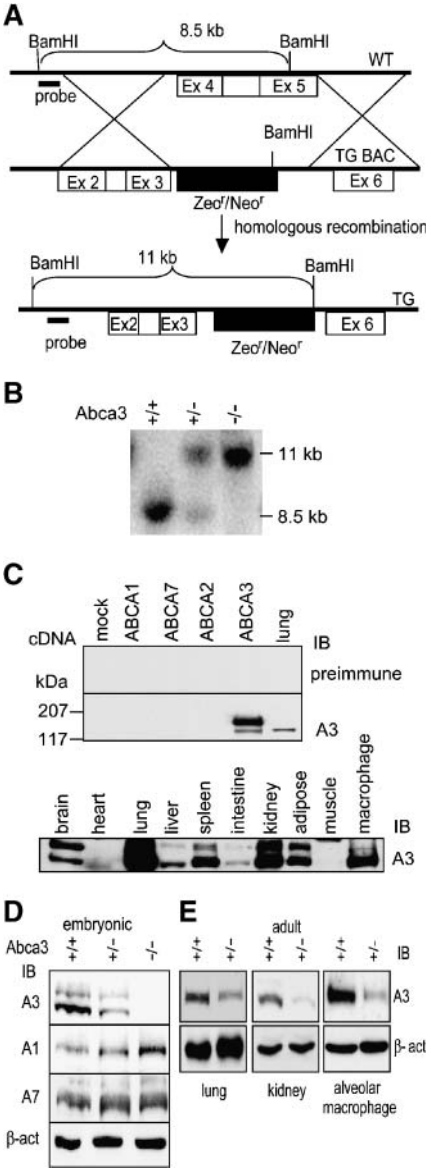

Fig. 1. Targeted deletion of *Abca3* results in neonatal lethality. A: Exons 4 and 5 of the *Abca3* wild-type locus (WT) were disrupted by homologous recombination using a targeted bacterial artificial chromosome (TG BAC). B: Southern analysis of DNA from day 18.5 embryos derived from $Abca3^{+/-}$ intercrosses shows transmission of the 11 kb targeted allele and generation of the null state. C: A rabbit anti-mouse ABCA3 antiserum was generated that detects a 180 kDa protein in 293 cells transfected with ABCA3 cDNA and does not cross-react with other A class transporters (top panels; 20 μg of total cellular protein). Immunoblotting (IB) of mouse tissues using this antibody demonstrated that ABCA3 protein is most highly expressed in the lung and moderately expressed in the kidney, adipose, macrophage, and spleen (bottom panel; 50 μg of total cellular protein). D: Embryonic $Abca3^{-/-}$ mice do not express ABCA3 protein. Immunoblotting of whole body lysates from wild-type, $Abca3^{+/-}$, and $Abca3^{-/-}$ day 18.5 embryos confirmed the loss of ABCA3 protein and revealed a mild upregulation of ABCA1, but not ABCA7, in these mice (40 μg of total protein). E: Diminished levels of ABCA3 protein are maintained in the adult heterozygous state as determined by immunoblotting of lung, kidney, and alveolar macrophage lysates from 12 week old $Abca3^{+/+}$ and $Abca3^{+/-}$ mice (lung sample, 15 μg of total protein and 10 s exposure; kidney samples, 20 μg of total protein and 30 s exposure; alveolar macrophage sample, 15 μg of total protein and 5 min exposure).

ture in the lungs of E18.5 embryos was assessed by smooth muscle actin staining using a commercially available antibody coupled to alkaline phosphatase (Sigma) and counterstaining with hematoxylin. The amount of SP-B secreted into the airspaces of E18.5 lungs was measured by staining E18.5 embryo lung sections for mature SP-B using a mouse anti-SP-B antibody (Abcam) and horseradish peroxidase detection. This antibody preferentially detects mature secreted SP-B. The amount of airspace SP-B staining was assessed by a blinded viewer using a Leica DMLB microscope interfaced with Leica Q Win 550 image-analysis softwear. A saccule airspace was considered positive for secreted SP-B if the airspace staining was clearly associated with acellular material that was not counterstained for nuclei with methyl green. Approximately 600 saccules were scored from three littermate-matched $Abca3^{+/+}$ and $Abca3^{-/-}$ samples. The percentage of SP-B-positive saccules was calculated, and the significance of the difference of positive saccules between genotypes was determined by a two-tailed Student's *t*-test.

Electron microscopy

Lungs were fixed overnight in 4% paraformaldehyde and 1% gluteraldehyde in 0.1 M cacodylate buffer, pH 7.4, at 4°C, rinsed in 0.1 M cacodylate buffer, and postfixed for 1 h in 1% OsO_4 in cacodylate buffer at room temperature. The samples were rinsed in buffer, then in distilled water, and stained en bloc in 2% aqueous uranyl acetate for 1 h. Samples were then rinsed in distilled water and dehydrated through a graded series of ethanol to 100%. Samples were infiltrated overnight on a shaker in a 1:1 solution of Epon-812 resin (Electron Microscopy Sciences) and 100% ethanol at room temperature. After further infiltration in 100% Epon-812, samples were embedded in fresh Epon-812 overnight at 60°C. Thin sections were cut on a Reichert Ultracut E ultramicrotome, collected onto formvar-coated slot grids, poststained with uranyl acetate and lead citrate, and imaged using a JEOL 1011 transmission electron microscope with an AMT digital camera at 80 kV (JEOL USA). An extensive survey of lamellar body formation and surfactant secretion in lung samples from littermate-paired E18.5 pups ($Abca3^{+/+}$ and $Abca3^{-/-}$; n = 5) was carried out on 128 micrographs at magnifications of 10,000–60,000.

Phospholipidomics

After homogenization by 20 strokes in a Dounce homogenizer in 0.4 ml of 1× PBS, total lipids were isolated from littermate-paired E18.5 embryo ($Abca3^{+/+}$ and $Abca3^{-/-}$; n = 5) lungs by one 2 ml extraction with chloroform-methanol (1:1, v/v) and two 0.5 ml chloroform extractions. The combined organic phases were washed once with 0.5 ml of KCl (1 M) and twice with 0.5 ml of water, dried under a stream of N_2 gas, and stored at −80°C until analysis. For phospholipid profiling, an automated electrospray ionization-tandem mass spectrometry approach was used, and data acquisition and analysis and acyl group identification were carried out as described previously with minor modifications (15, 16). The dried extracts were resuspended in chloroform, and an aliquot of extract (30 μl out of 1 ml) was taken for mass spectrometry analysis. The lipid extract was combined with solvents and internal standards, such that the ratio of chloroform-methanol-300 mM ammonium acetate in water was 300:665:35, and the final volume was 1.23 ml. Internal standards, obtained and quantified as described previously (16), were 0.66 nmol of di14:0-PC, 0.66 nmol of di24:1-PC, 0.66 nmol of 13:0-lyso PC, 0.66 nmol of 19:0-lyso PC, 0.36 nmol of di14:0-phosphatidylethanolamine (PE), 0.36 nmol of di24:1-PE, 0.36 nmol of 14:0-lyso PE, 0.36 nmol of 18:0-lyso PE, 0.36 nmol of di14:0-PG, 0.36 nmol of di24:1-PG, 0.36 nmol of 14:0-lyso PG, 0.36 nmol of 18:0-lyso PG, 0.24 nmol of di14:0-phosphatidylserine (PS), 0.24 nmol of

di20:0(phytanoyl)-PS, 0.20 nmol of 16:0-18:0-phosphatidylinositol (PI), and 0.16 nmol of di18:0-PI. Unfractionated lipid extracts were introduced by continuous infusion into the electrospray ionization source on a triple quadrupole tandem mass spectrometer (API 4000; Applied Biosystems, Foster City, CA). Samples were introduced using an autosampler (LC Mini PAL; CTC Analytics AG, Zwingen, Switzerland) fitted with a 1 ml injection loop and presented to the electrospray ionization needle at 30 μl/min. The collision gas pressure was set at 2 (arbitrary units) for phospholipids. The collision energies, with nitrogen in the collision cell, were 28 V for PE, 40 V for PC and SM, −58 V for PI, −57 V for PG, and −34 V for PS. Declustering potentials were 100 V for PE, SM, and PC and −100 V for PG and PI. Entrance potentials were 15 V for PE, 14 V for PC and SM, and −10 V for PI, PG, and PS. Exit potentials were 11 V for PE, 14 V for PC, −15 V for PI, −14 V for PG, and −13 V for PS. The mass analyzers were adjusted to a resolution of 0.7 units full width at half height. For each spectrum, 9–150 continuum scans were averaged in multiple channel analyzer mode. The source temperature (heated nebulizer) was 100°C, the interface heater was on, +5.5 kV or −4.5 kV was applied to the electrospray capillary, the curtain gas was set at 20 (arbitrary units), and the two ion source gases were set at 45 (arbitrary units).

Lipid species were detected, using the scans described previously, including neutral loss of 87 in the negative mode for PS (16, 17). Sequential precursor and neutral loss scans of the extracts produce a series of spectra with each spectrum revealing a set of lipid species containing a common head group fragment. SM was determined from the same mass spectrum as PC (precursors of *m/z* 184 in positive mode) (17, 18) and by comparison with PC internal standards using a molar response factor for SM (compared with PC) determined experimentally to be 0.37. The background of each spectrum was subtracted, the data were smoothed, and peak areas were integrated using a custom script and Applied Biosystems Analyst software. Isotopic overlap corrections were applied, and the lipids in each class were quantified compared with the two internal standards of that class using standard curve shapes determined for the API 4000 mass spectrometer.

Individual acyl group identification

The acyl groups of PC and PG species found to be significantly affected by the loss of ABCA3 expression were identified as acyl anions from the appropriate negative ion precursors. The collision energies were 20–55 V. The solvent was chloroform-methanol-300 mM ammonium acetate in water (300:665:35). PG was analyzed as $[M - H]^-$, and PC was analyzed as $[M + OAc]^-$.

Cholesterol and triglyceride analysis

Oil Red O staining of 4% paraformaldehyde-fixed frozen lung sections was used to assess the distribution and levels of cholesterol and triglycerides in littermate E18.5 $Abca3^{+/+}$ and $Abca3^{-/-}$ embryos as described previously (19). Total cholesterol, triglyceride, and free glycerol levels were determined on lung lipid extracts by enzymatic assays using commercially available reagents (Sigma-Aldrich) by the method of Carr, Andresen, and Rudel (20). Cholesterol efflux assays were carried out as described previously (12). In brief, 293-EBNA-T cells were seeded onto 24-well poly-D-lysine-coated tissue culture plates at 100,000 cells/well and 72 h later were transfected in triplicate with empty vector or the indicated cDNAs using Lipofectamine 2000 (Invitrogen). Twenty-four hours after transfection, the cells were incubated with 0.5 μCi/ml [^{3}H]cholesterol in complete medium (10% FBS/DMEM) for 24 h. Non-cell-associated cholesterol was removed by two washes with 1× PBS, a 2 h incubation in medium at 37°C, and two additional washes in 1× PBS. The cells were further incubated in medium alone (1 mg/ml fatty acid-free BSA/DMEM) or in medium with 10 μg/ml delipidated apolipoprotein A-I (apoA-I) for 12 h. Medium was collected from the cells and cleared of debris by an 800 *g* spin for 10 min. To calculate total cholesterol uptake and efflux, the cell layers were dissolved in 0.1 N NaOH, and the amount of radioactivity in the medium and cell lysates was measured by scintillation counting. Total cell-associated cholesterol was expressed as cpm/well. ApoA-I dependent cholesterol efflux was expressed as the percentage of efflux [medium cpm/(medium + cell cpm) × 100] for the apoA-I-treated cells minus the percentage of efflux from the cells treated with medium alone.

Statistical analysis

Data sets were tested for equal variance and, when found to have equal variance, were further compared by a two-tailed Student's *t*-test using the SigmaStat software package. The lung weights of the adult wild-type and $Abca3^{+/-}$ mice were found to have unequal variance; thus, the lung weights were first transformed to their natural logarithm before being compared by a two-tailed Student's *t*-test. Statistical significance was defined as $P < 0.05$.

RESULTS

Homozygous null Abca3 mutations in mice result in neonatal lethality

Recombination of the *Abca3* locus was accomplished by electroporating a BAC lacking exons 4 and 5 into 129/SvEv embryonal stem cells (Fig. 1A) (13). Injection of targeted ES cells generated two chimeric lines, one of which transmitted the targeted allele to F1 progeny. Southern analysis of DNA from late-term embryos (E15.5–18.5) derived from $Abca3^{+/-}$ intercrosses demonstrated transmission of the 11 kb targeted allele at the expected Mendelian frequencies (Fig. 1B; wild type-heterozygous-null embryo ratio of 51:102:52); however, no homozygous null animals survived the immediate postnatal period. Thus, deletion of ABCA3 in the mouse results in neonatal lethality, consistent with the hypothesis that the ABCA3 transport function is essential for respiratory function.

To characterize the defect in these mice further, we generated an anti-ABCA3 antibody that lacked cross-reactivity to other ABCA class members, including A1, A2, and A7 (Fig. 1C). In 293 cells transfected with an ABCA3 cDNA, the antibody detected two bands, the lower of which co-migrated with the predominant ABCA3 isoform expressed in murine lung. We then analyzed the expression of ABCA3 in adult mouse tissues by immunoblot (Fig. 1C, lower panel). As has been reported for ABCA3 mRNA in the rat, ABCA3 protein expression was highest in mouse lung, with moderate expression in the kidney (9). Other tissues that demonstrated substantial expression included brain, white adipose tissue, and bone marrow-derived macrophages. Immunoblotting whole embryo lysates of $Abca3^{-/-}$ mice confirmed the loss of ABCA3 protein in these animals, whereas heterozygous embryos exhibited ABCA3 protein levels approximately half those of wild-type mice (Fig. 1D). Evaluation of other ABCA transporters in these mice re-

TABLE 1. Body, lung, and kidney weights of adult wild-type and Abca3$^{+/-}$ mice at 4 months of age

Sample	Abca3$^{+/+}$	Abca3$^{+/-}$	*P*
Body	38.2 ± 5.2 (18)	39.8 ± 5.1 (27)	0.31
Lung	0.39 ± 0.04 (16)	0.40 ± 0.08 (24)	0.54
Kidney	0.50 ± 0.07 (15)	0.53 ± 0.09 (24)	0.41

Body and tissue weights are in grams ± SD. Sample numbers are in parentheses. *P* values are derived from a two-tailed Student's *t*-test.

vealed that ABCA1 was modestly upregulated in *Abca3*$^{-/-}$ mice and that the expression of ABCA7 was unchanged. Compared with age-matched wild-type animals, 12 week old heterozygous mice continued to demonstrate reduced expression of ABCA3 protein in lung and kidney tissues as well as in alveolar macrophages (Fig. 1E). The body weights, as well as lung and kidney weights, in the adult *Abca3*$^{+/-}$ mice were statistically indistinguishable from those of their wild-type littermates (**Table 1**). These data indicate that mice whose expression of ABCA3 is reduced by approximately half develop and grow normally and are able to survive into adulthood.

Abca3$^{-/-}$ mice display normal embryonic development but fail to inflate their lungs upon birth

To assess the cause of death of *Abca3*$^{-/-}$ pups, studies were performed on late-stage embryos as well as neonates. Gross examinations of day 18.5 embryos obtained by cesarean section showed the null embryos to be normally developed, with total body, lung, and kidney weights statistically indistinguishable from those of the wild-type or heterozygous embryos (**Table 2**). Histologic analysis of E18.5 lung tissue also showed grossly normal architecture (**Fig. 2A**), although a slight trend toward reduced alveolar chord length in the null tissues was noted [*Abca3*$^{+/+}$, 9.96 ± 2.15 μm (n = 6); *Abca3*$^{-/-}$, 7.34 ± 2.12 μm (n = 5); *P* = 0.7]. However, staining of the lung tissue for α smooth muscle actin indicated that the airways and pulmonary vasculature had developed normally in the absence of ABCA3 (see supplementary Fig. I). Finally, loss of ABCA3 expression in the E18.5 kidneys also resulted in no grossly discernible abnormalities (Fig. 2A). Thus, complete loss of ABCA3 in mice does not appear to affect in utero development as detected by light microscopy.

Next, litters resulting from crosses of heterozygous animals were allowed to develop to term, and newborn pups were observed for signs of distress immediately after birth. *Abca3*$^{-/-}$ pups were born with initially normal color and exhibited typical early motor activity, including concerted efforts to breathe (see supplementary video). However, soon after birth, the null pups became lethargic and cyanotic and failed to nurse. Inflation of the lungs and oxygenation of the blood, evident in the development of a pulsating white patch in the thoracic region of wild-type and heterozygous mice, never occurred in *Abca3*$^{-/-}$ pups

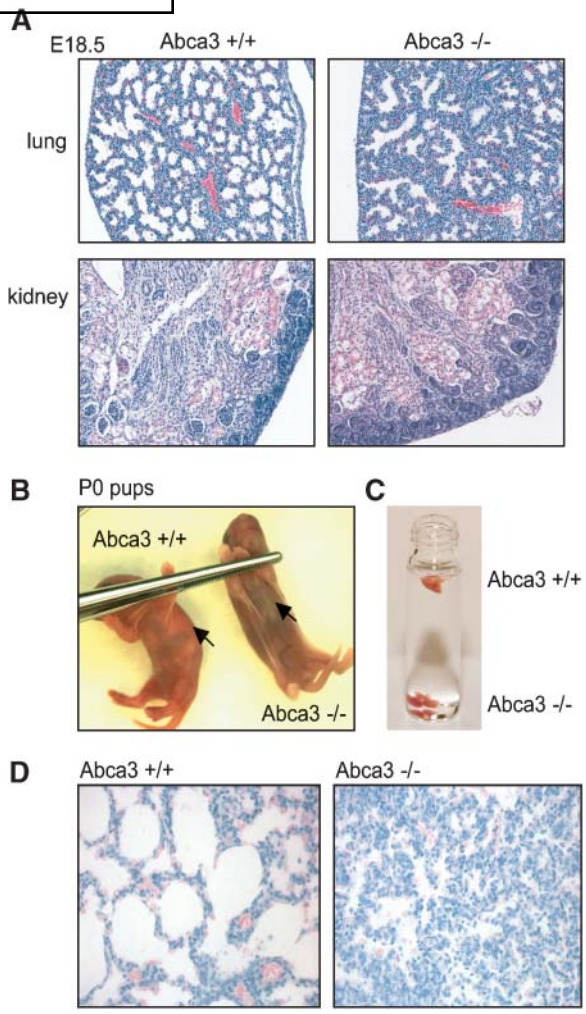

Fig. 2. *Abca3*$^{-/-}$ mice suffer fatal neonatal respiratory distress. A: Hematoxylin/eosin stains of tissues from day 18.5 wild-type and *Abca3*$^{-/-}$ mice reveal no gross abnormalities in lung or kidney structure (20×). B: At birth, *Abca3*$^{-/-}$ pups attempt breathing movements but fail to inflate their lungs, rapidly becoming cyanotic and then inactive (arrows indicate the inflated lungs of the of the *Abca3*$^{+/+}$ pup that are lacking in the *Abca3*$^{-/-}$ pup). C: The lungs from *Abca3*$^{-/-}$ pups sink in phosphate-buffered saline, confirming a lack of inflation. D: Hematoxylin/eosin-stained lung sections show collapsed airspaces in the lungs of the P0 *Abca3*$^{-/-}$ pups (40×).

TABLE 2. Body, lung, and kidney weights of embryonic day 18.5 wild-type, Abca3$^{+/-}$, and Abca3$^{-/-}$ mice

Sample	Abca3$^{+/+}$	Abca3$^{+/-}$	Abca3$^{-/-}$	*P*
Total body	1.307 ± 0.17 (8)	1.23 ± 0.14 (18)	1.29 ± 0.11 (11)	0.26, 0.81
Lungs	0.037 ± 0.005 (14)	0.039 ± 0.005 (19)	0.043 ± 0.005 (17)	0.4, 0.1
Kidney	0.009 ± 0.0014 (8)	0.009 ± 0.0019 (11)	0.009 ± 0.002 (6)	0.44, 0.46

Body and tissue weights are in grams ± SD. Sample numbers are in parentheses. *P* values are derived from a two-tailed Student's *t*-test comparing the Abca3$^{+/+}$ values with either the Abca3$^{+/-}$ or Abca3$^{-/-}$ values.

(Fig. 2B). All *Abca3*$^{-/-}$ pups ceased activity and died within 10–60 min after birth. Analysis of the lungs of *Abca3*$^{-/-}$ mice indicated that the primary cause of death was atelectasis, or collapse of the alveolar space. This was grossly apparent in that *Abca3*$^{-/-}$ lungs contained little or no air and sank when placed in phosphate-buffered saline (Fig. 2C), a finding consistent with the histologic evidence of no inflated airspaces in the *Abca3*$^{-/-}$ lungs (Fig. 2D).

Abca3$^{-/-}$ lungs lack secreted surfactant and mature lamellar bodies

As pulmonary surfactant is critical for lung inflation and the maintenance of the alveolar space, electron microscopy was used to test whether the loss of ABCA3 activity disrupted surfactant production. Micrographs of lungs from an *Abca3*$^{-/-}$ P0 mouse exhibited little or no secreted surfactant, compared with the lungs of a littermate *Abca3*$^{+/+}$ mouse (**Fig. 3A**, arrows point to secreted surfactant in the airspaces of the wild-type lung). Along with the lack of surfactant, the null lung exhibited tissue damage and leakage of red blood cells into the collapsed airspaces (Fig. 3A, arrowhead). To avoid the potential of postmortem tissue damage artifacts, the lungs of E18.5 embryos delivered by cesarean section were examined further. Additionally, because ABCA3 mutations in humans have been reported to have a variable impact on lamellar body structure, a more extensive analysis of 128 micrographs of five littermate-paired lung samples was undertaken. In wild-type mice, secreted surfactant and normal surfactant storage organelles, with their characteristic internal lamellae (lamellar bodies), were consistently observed throughout the lung tissue (Fig. 3B, arrows point to lamellar bodies). In contrast, the lungs of *Abca3*$^{-/-}$ embryos again showed little or no secreted surfactant and lacked mature lamellar bodies, although the lamellae precursor multivesicular bodies appeared to be normal (Fig. 3B). These results suggested that loss of ABCA3 produced a strong block in the secretion of surfactant. Because the hydrophobic surfactant protein B is also stored in lamellar bodies and is cosecreted with surfactant lipids, we analyzed whether the loss of ABCA3 activity was also associated with a block in the secretion of SP-B. This was found to be the case in that immunostaining of wild-type and Abca3$^{-/-}$ lungs from E18.5 embryos revealed dramatically less mature SP-B staining in the airspaces of the Abca3$^{-/-}$ lungs, whereas intracellular staining was largely unchanged (see supplementary Fig. IIIA, arrows point to airspace staining that is not cell-associated, as assessed by the lack of counterstaining with methyl green). Blinded counts of three samples from littermate-paired animals showed a significant 95% reduction in the number of airspaces stained positive for SP-B in the Abca3$^{-/-}$ lungs (see supplementary Fig. IIIB). In composite, these results indicate that ABCA3 activity is critical for the formation of lamellar bodies and the secretion of surfactant.

Phospholipid profiling indicates that ABCA3 activity maintains PG levels in the lung

To date, mutations in transporters of the ABCA class have been associated with prominent disruptions in lipid homeostasis, suggesting that all members of this class may play a role in lipid transport. Profiling of lipid classes by mass spectrometry is a recently developed technique that permits a more global analysis of tissues for changes in

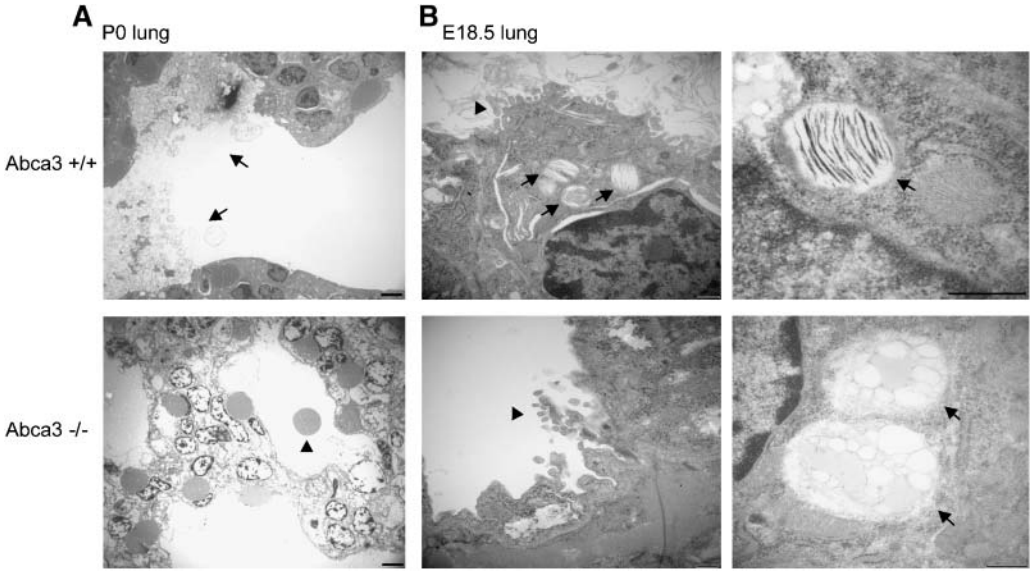

Fig. 3. *Abca3*$^{-/-}$ lungs lack secreted surfactant and mature lamellar storage bodies. A: Electron micrographs of lungs from P0 pups demonstrate secreted surfactant (arrows) in the alveolus of an *Abca3*$^{+/+}$ mouse that is lacking in the *Abca3*$^{-/-}$ sample (bars = 3.7 μm; the arrowhead points to a red blood cell in the *Abca3*$^{-/-}$ alveolus). B: E18.5 *Abca3*$^{+/+}$ lungs show copious secreted surfactant and mature lamellar bodies that are lacking in the *Abca3*$^{-/-}$ lung (bar = 500 nm; arrows point to lamellar bodies in the *Abca3*$^{+/+}$ lung and a multivesicular body in the *Abca3*$^{-/-}$ lung; arrowheads point to microvilli on type II cells).

their lipid composition. As surfactant is principally composed of phospholipids, and loss of ABCA3 in our mice appeared to have strongly disrupted the storage and secretion of surfactant, we used mass spectrometry to profile the phospholipid content of lung tissue derived from littermate paired P0 pups (n = 5). We analyzed 333 individual species covering the major phospholipids as well as their lyso and ether derivatives (see supplementary Table I). The total phospholipid mass per gram of lung tissue did not differ significantly between the genotypes, although a trend for the null lungs to have less phospholipid was evident (**Table 3**). In contrast, the null lungs showed an 85% reduction in the mass of PG, whereas the other major phospholipid classes did not differ significantly (Table 3). However, when analyzing individual PG and PC subspecies, additional differences were observed. The reduction in PG mass was accompanied by decreases across all of the major subspecies of PG detected in this assay, including PG 34:1 (**Fig. 4A**). In contrast, for PC, shorter acyl chain species were reduced in the *Abca3*$^{-/-}$ lungs, but PC 34:1 along with other longer chain species were not significantly different in the varying mouse genotypes (Fig. 4B, C). The acyl groups of the PC and PG species found to be significantly reduced by the loss of ABCA3 expression were identified as acyl anions from the appropriate negative ion precursors. As expected, the PC and PG 32:0 species contained only fully saturated palmitoyl chains (16:0), the 32:1 species contained palmitoyl and palmitoleoyl chains (16:0 and 16:1, respectively), and the 34:1 species contained palmitoyl and oleoyl chains (16:0 and 18:1, respectively).

For PS, PE, PI, and SM, no significant differences were found among the major species, although a few minor species were also found to be lower in the Abca3$^{-/-}$ samples, including PE 36:6, PI 36:3, and PI 40:7 (**Fig. 5A–D**). In composite, these data indicate that ABCA3 activity is most important for maintaining lung levels of PG and, to a lesser degree, the level of PC species with short acyl chains.

Loss of ABCA3 activity does not influence lung cholesterol levels

As lamellar bodies and surfactant also contain cholesterol, and in vitro assays by Cheong et al. (11) have suggested that ABCA3 can stimulate the cellular uptake of cholesterol, we sought to assess whether cholesterol homeostasis had been disrupted in the Abca3$^{-/-}$ lung. Staining frozen lung sections with Oil Red O, which detects cholesterol as well as other neutral lipids, did not indicate that the loss of ABCA3 had a major effect on the levels of these lipids, although staining in the null tissue was slightly more diffuse, consistent with a disruption of lamellar bodies (data not shown). Cholesterol levels were measured in Abca3$^{+/+}$ and Abca3$^{-/-}$ lungs by enzymatic assays, further confirming that loss of ABCA3 activity did not significantly alter the amount of this neutral sterol (**Fig. 6A**). Although total lung cholesterol levels were not prominently altered by the loss of ABCA3 expression, the disruption of lamellar body structure may have altered the cellular distribution of cholesterol and could have been responsible for the slight upregulation of ABCA1 expression that was seen in whole embryo lysates of the Abca3$^{-/-}$ mice (Fig. 1D). However, immunoblots showed the levels of ABCA1 protein in the lungs of Abca3$^{-/-}$ mice to be similar to the levels in the lungs of wild-type mice, whereas a slight increase in ABCA1 protein was again detected in the brain of Abca3$^{-/-}$ mice (see supplementary Fig. IV). Finally, although 293-EBNA-T cells transfected with the mouse ABCA3 cDNA led to robust expression of transporter (Fig. 6B), these cells were not found to accumulate greater amounts of tritiated cholesterol than cells that were mock-transfected (Fig. 6C). The ability of the ABCA3 transfected cells to efflux cholesterol to apoA-I was additionally measured in these assays and compared with the efflux activity of ABCA1 transfected cells. ABCA3 expression did not significantly alter this cholesterol-trafficking process (Fig. 6D). In composite, our experiments do not indicate a prominent role for ABCA3 in maintaining lung cholesterol homeostasis, although they do not rule out more subtle effects on sterol trafficking in the lung and other tissues, such as the brain.

TABLE 3. Lung phospholipid contents of embryonic day 18.5 wild-type and Abca3$^{-/-}$ mice

Phospholipid	Abca3$^{+/+}$	Abca3$^{-/-}$	*P*
Phosphatidylglycerol	191 ± 50	30 ± 9	0.01
Phosphatidylcholine	2,265 ± 192	1,636 ± 356	0.16
Phosphatidylserine	386 ± 44	351 ± 78	0.71
Phosphatidylethanolamine	1,027 ± 132	801 ± 176	0.33
Phosphatidylinositol	225 ± 31	194 ± 56	0.64
Sphingomyelin	430 ± 40	372 ± 83	0.55
Total phospholipid	4,526 ± 456	3,384 ± 751	0.23

Phospholipid masses are in nmol/g lung tissues ± SEM (n = 5). *P* values are derived from a two-tailed Student's *t*-test.

DISCUSSION

This work demonstrates that *Abca3*$^{-/-}$ mice die of respiratory failure as a result of an inability to secrete pulmonary surfactant into the alveolar space. The phenotype is completely penetrant in that all of the *Abca3*$^{-/-}$ pups died within 1 h of birth, having failed to inflate their lungs. These results indicate that ABCA3 transport function is essential for mammals to transition to air respiration. In contrast to our mouse model, children with ABCA3 genetic mutations who developed neonatal respiratory distress showed a more variable disease course and time of death (6, 8), perhaps because their mutant transporters retained some functional activity. Indeed, a more recent report suggests that compound missense ABCA3 mutations are associated with chronic lung disease that is compatible with survival into adulthood (7). Our results make clear that some ABCA3 activity is required for respiratory function and survival. The insertion of hypomorphic ABCA3 alleles into the null animals may provide additional useful models to study the pathogenesis of more commonly occurring respiratory disorders that have been suggested by the recent human genetic association data.

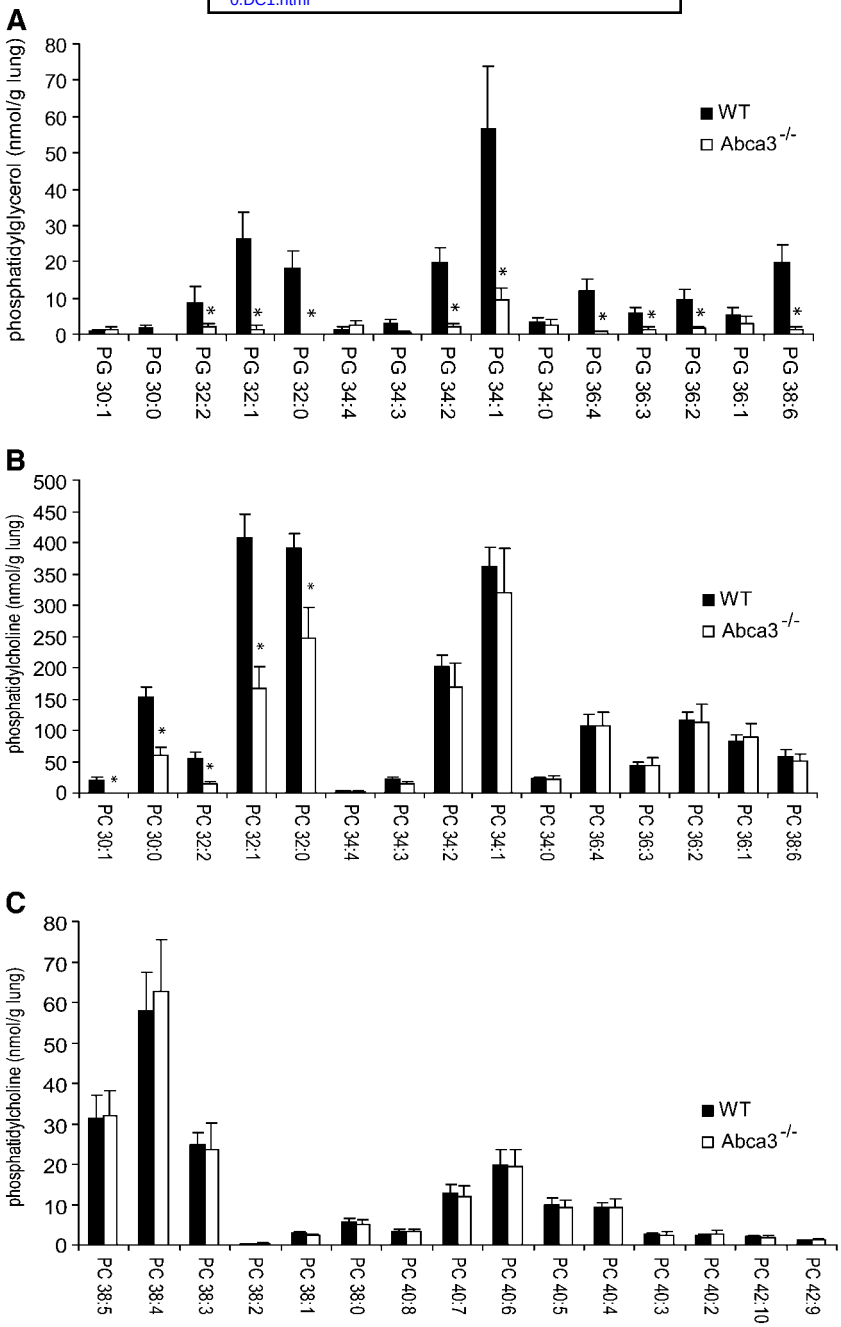

Fig. 4. Phosphatidylglycerol (PG) levels are depleted in *Abca3*$^{-/-}$ lungs. Organic lipid extracts from littermate *Abca3*$^{+/+}$ and *Abca3*$^{-/-}$ lungs were profiled for phospholipid content by electrospray ionization-tandem mass spectrometry and expressed as nanomoles of the indicated phospholipid species per gram of lung tissue (n = 5; ±SEM; * $P < 0.05$). The total acyl carbon:total double bond content of each phospholipid species is indicated on the *x* axis. A: PG levels including PG 34:1 and PG 34:2 are significantly depleted in *Abca3*$^{-/-}$ lungs. B, C: Phosphatidylcholine (PC) species with short acyl chains are selectively depleted in the *Abca3*$^{-/-}$ lungs. WT, wild type.

Why is ABCA3 function critical for lung function and the generation of surfactant? The alveolus of the mammalian lung dynamically expands and contracts during the respiratory cycle. During expiration, as the alveoli contract, the surface tension generated by the aqueous hypophase lining the airspaces can cause their collapse. To reduce surface tension and prevent collapse, type II alveolar cells secrete surfactant, a mixture composed primarily of phospholipid with lesser amounts of cholesterol and hydrophobic proteins. Here, we show that the formation of the lamellar body, which stores surfactant before its release into the alveolus, is severely disrupted in mice lacking ABCA3 activity. In contrast to this nearly complete disruption of lamellar body structure, various human ABCA3 mutations have been associated with a more variable impact on lamellar body structure (6, 8).

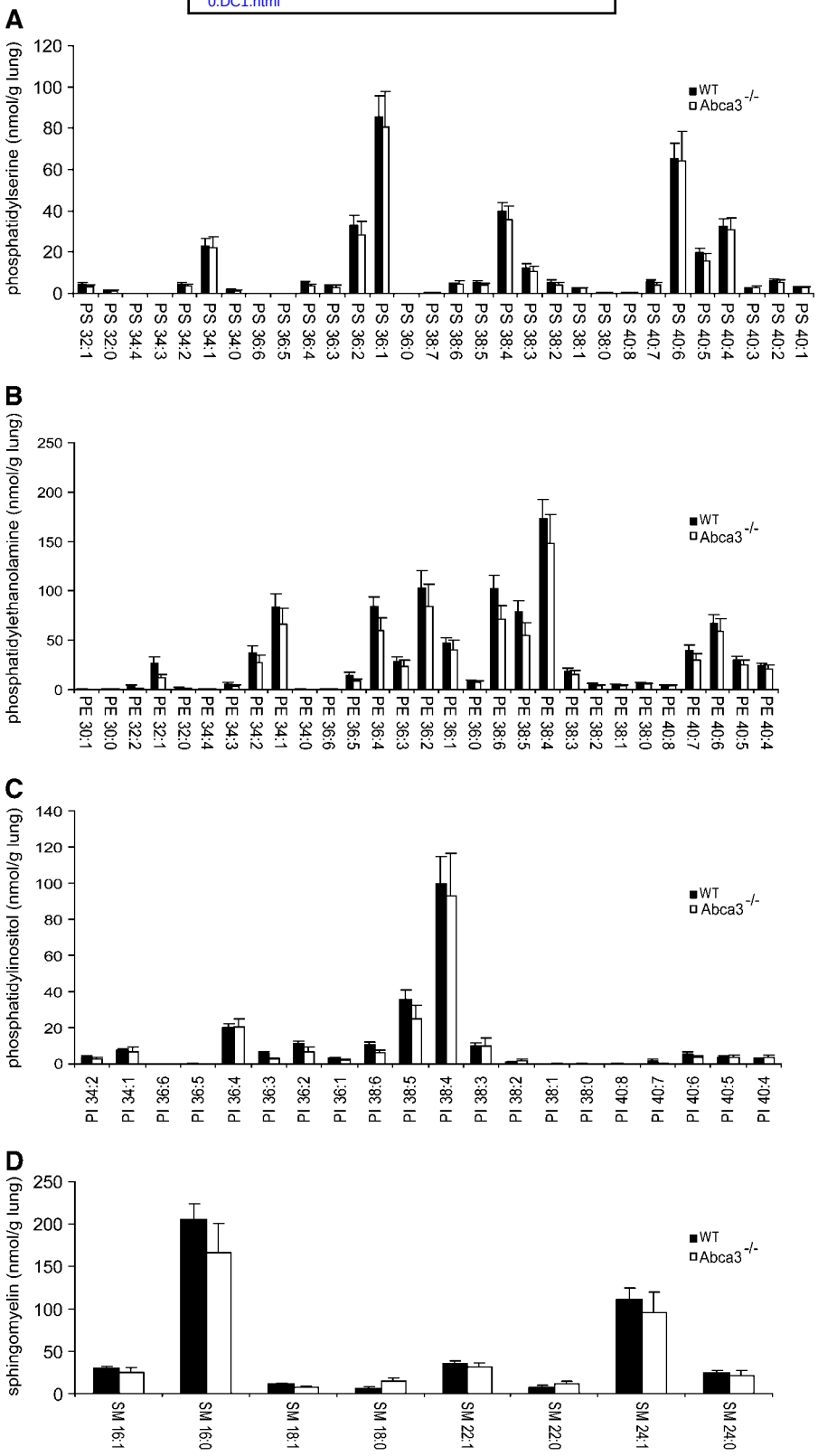

Fig. 5. Loss of ABCA3 activity does not disrupt lung levels of the other major phospholipids. Organic lipid extracts from E18.5 littermate $Abca3^{+/+}$ and $Abca3^{-/-}$ lungs were profiled for phospholipid content by electrospray ionization-tandem mass spectrometry and expressed as nanomoles of the indicated phospholid species per gram of lung tissue (n = 5; ±SEM). The total acyl carbon:total double bond content of each phospholipid species is indicated on the *x* axis. A: Phosphatidylserine (PS) levels. B: Phosphatidylethanolamine (PE) levels. C: Phosphatidylinositol (PI) levels. D: Sphingomyelin (SM) levels.

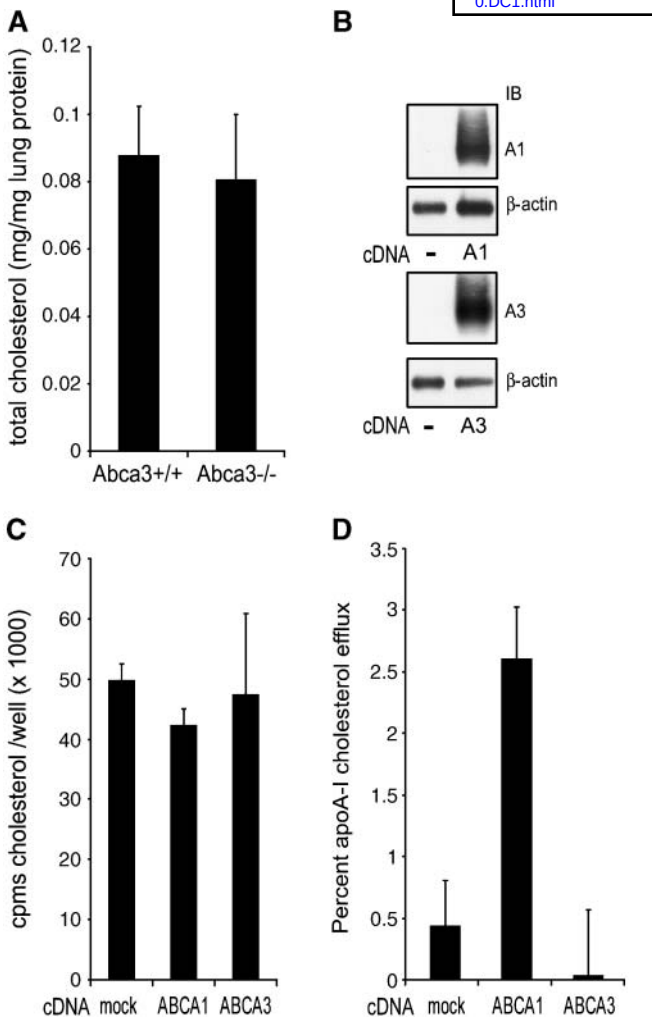

Fig. 6. Loss of ABCA3 does not significantly disrupt lung cholesterol homeostasis. A: Enzymatic quantification of total lung cholesterol showed no significant differences between E18.5 littermate-matched *Abca3*$^{+/+}$ and *Abca3*$^{-/-}$ lungs (n = 5; ±SD; $P = 0.53$). Forced expression of ABCA3 in 293-EBNA-T cells does not stimulate the uptake of radiolabeled cholesterol or modulate efflux to apolipoprotein A-I (apoA-I). B: Immunoblots (IB) demonstrate significant ABCA1 and ABCA3 expression in 293-EBNA-T cells after transfection with the respective cDNAs. C, D: Uptake of [^{3}H]cholesterol by these ABCA3 transfected cells was not significantly different (C) (n = 3; ±SD; $P = 0.78$), and only the ABCA1 transfected cells significantly stimulated efflux to apoA-I (D) (n = 3; ±SD; $P = 0.005$).

This again may reflect differences in residual ABCA3 transport function among the various mutations identified and possibly in the ability of the mutant transporters to localize to the lamellar body (11, 21). Our results shows that in mice completely lacking ABCA3 protein, the transporter's function is essential for the formation of the lamellar body and for surfactant release into the airspaces.

How the absent lamellar body structure and surfactant secretion relates to ABCA3 transport activity is less clear. Because other close homologs of ABCA3 are known to stimulate the movement of lipids across membrane bilayers, it is reasonable to suspect that ABCA3 may also possess such activity. Indeed, Cheong et al. (11) have suggested that ABCA3 has a broad transport capacity that stimulates the cellular uptake of PC, SM, and cholesterol, as determined by in vitro assays using microscopy and uptake of fluorescent lipid analogs. This suggests an ABCA3 transport activity similar in nature, but opposite in direction, to that of ABCA1, a homolog of ABCA3. However, our analysis of the cholesterol levels in lungs of Abca3$^{-/-}$ mice did not indicate a major change in the levels of this lipid, and we found that forced expression of ABCA3 in 293 cells did not stimulate the uptake or inhibit the release of radiolabeled cholesterol. These experiments make it less likely that ABCA3 plays a major role in cholesterol homeostasis, but they do not exclude a more subtle role in sterol trafficking, as suggested by the results of Cheong et al. (11). As with cholesterol, our results indicate that lung triglyceride and free glycerol were also not strongly dependent on ABCA3 activity (data not shown). In contrast, our mass spectrometry profiling of the null lungs did reveal a more specialized role for ABCA3 in the metabolism of PG and short acyl-chained PC species. To our knowledge, this is first description of an ABC transporter that has such a restricted and dramatic effect on tissue PG levels (22–24). This finding highlights the utility of profiling lipid levels by mass spectrometry and suggests that the method may help identify the transport function of other poorly characterized ABCA transporters. It also provides a mechanistic rationale for the use of clinical assays that measure PG levels in amniotic fluids as a metabolic marker of lung maturity.

PG is uniquely enriched in the lung and constitutes ~10% of the phospholipid content in secreted surfactant. PC constitutes up to 80% of the phospholipid content in surfactant, and of this, nearly 40% is dipalmitoyl PC (PC 32:0), whereas palmitoyloleoyl PC (PC 32:1), at 25%, is the next most abundant surfactant PC species in the mouse (25) (M. L. Fitzgerald and M. W. Freeman, unpublished observations). The loss of ABCA3 activity prominently affected the level of these PC species as well as levels of PC 32:2, PC 30:1, and PC 30:0. However, PC 34:1 and the other major PC species with longer acyl chains were not reduced significantly. In contrast, PG 34:1, and all other major PG species, were reduced, thus significantly decreasing total PG levels in the lung. Surfactant PG stored in lamellar bodies contains a broad range of acyl chain species, and this pool encompasses the majority of the lung PG (26). In contrast, surfactant PC is restricted at birth to short acyl chain species, and this pool of PC constitutes a much smaller fraction of total lung PC (27). Our results indicate that the loss of ABCA3 activity selectively affected the metabolism of those phospholipids preferentially stored in lamellar bodies. It is these phospholipids, especially the unsaturated species, that play a critical role in reducing surface tension within the alveolus. That these phospholipids are specific and direct transport substrates for ABCA3, dependent on the transporter for accumulation in the lamellar body, is suggested by our results. Alternatively, the loss of ABCA3 activity could disrupt lamellar body formation by another mechanism, thus lead-

ing to a decrease in specific stored phospholipids by a secondary feedback mechanism.

In conclusion, the generation of Abca3 null mice has established an essential role for this transporter in the formation of pulmonary lamellar bodies and the secretion of surfactant from alveolar type II cells. The loss of transporter function results in neonatal respiratory failure and death, as is seen in humans with some mutations in the ABCA3 gene. The transporter plays a critical role in the accumulation of PG in murine lung tissue at birth, suggesting that it plays a key role in the transport of this phospholipid into the lamellar body. This work also provides additional evidence that strengthens the hypothesis that all members of the ABCA class of transporters will be involved in cellular lipid transport. Interestingly, mutation of the amphipathic helical surfactant protein B in humans and mice is also associated with neonatal respiratory distress, depletion of lung PG, and disruption of lamellar body structure, a phenotype remarkably similar to what we have observed in the Abca3 null mice (28, 29). Thus, although we do not provide direct evidence for the mechanism of lipid transport, our results suggest the intriguing possibility that the general process of ABCA-mediated cellular lipid export may share the common feature of loading intracellular lipid onto a specific amphipathic helical carrier protein, such as surfactant protein B (ABCA3) or apoA-I (ABCA1).

The authors thank Dr. Kathryn J. Moore (Lipid Metabolism Unit) for helpful discussions and critical reading of the manuscript, Dr. Dennis Brown (Program in Membrane Biology) for electron microscopy support, Derwin Hyde (Center for Computational and Integrative Biology) for photography support, and Mary Roth for mass spectrometry support. This work was funded by grants from the National Institutes of Health to M.W.F. (HL-68988, HL-45098, and HL-72358) and to M.L.F (HL-074136). The electron microscopy core is supported by an Inflammatory Bowel Disease Grant (DK-43351) and a Boston Area Diabetes and Endocrinology Research Center Award (DK-57521). The Kansas Lipidomics Research Center was supported by National Science Foundation Grants MCB 0455318 and DBI 0521587 and National Science Foundation EPSCoR Grant EPS-0236913, with matching support from the State of Kansas through the Kansas Technology Enterprise Corporation and Kansas State University. The Kansas Lipidomics Research Center also acknowledges support from Kansas-IDeA Networks of Biomedical Research Excellence from National Institutes of Health Grant P20 RR-16475 from the IDeA Networks of Biomedial Research program of the National Center for Research Resources.

REFERENCES

1. Dean, M., and T. Annilo. 2005. Evolution of the ATP-binding cassette (ABC) transporter superfamily in vertebrates. *Annu. Rev. Genomics Hum. Genet.* **6:** 123–142.
2. Brooks-Wilson, A., M. Marcil, S. M. Clee, L. H. Zhang, K. Roomp, M. van Dam, L. Yu, C. Brewer, J. A. Collins, H. O. Molhuizen, et al. 1999. Mutations in ABC1 in Tangier disease and familial high-density lipoprotein deficiency. *Nat. Genet.* **22:** 336–345.
3. Allikmets, R., N. F. Shroyer, N. Singh, J. M. Seddon, R. A. Lewis, P. S. Bernstein, A. Peiffer, N. A. Zabriskie, Y. Li, A. Hutchinson, et al. 1997. Mutation of the Stargardt disease gene (ABCR) in age-related macular degeneration. *Science.* **277:** 1805–1807.
4. Allikmets, R., N. Singh, H. Sun, N. F. Shroyer, A. Hutchinson, A. Chidambaram, B. Gerrard, L. Baird, D. Stauffer, A. Peiffer, et al. 1997. A photoreceptor cell-specific ATP-binding transporter gene (ABCR) is mutated in recessive Stargardt macular dystrophy. *Nat. Genet.* **15:** 236–246.
5. Akiyama, M., Y. Sugiyama-Nakagiri, K. Sakai, J. R. McMillan, M. Goto, K. Arita, Y. Tsuji-Abe, N. Tabata, K. Matsuoka, R. Sasaki, et al. 2005. Mutations in lipid transporter ABCA12 in harlequin ichthyosis and functional recovery by corrective gene transfer. *J. Clin. Invest.* **115:** 1777–1784.
6. Brasch, F., S. Schimanski, C. Muhlfeld, S. Barlage, T. Langmann, C. Aslanidis, A. Boettcher, A. Dada, H. Schroten, E. Mildenberger, et al. 2006. Alteration of the pulmonary surfactant system in full-term infants with hereditary ABCA3 deficiency. *Am. J. Respir. Crit. Care Med.* **174:** 571–580.
7. Bullard, J. E., S. E. Wert, J. A. Whitsett, M. Dean, and N. M. Nogee. 2005. ABCA3 mutations associated with pediatric interstitial lung disease. *Am. J. Respir. Crit. Care Med.* **172:** 1026–1031.
8. Shulenin, S., N. M. Nogee, T. Annilo, S. E. Wert, J. A. Whitsett, and M. Dean. 2004. ABCA3 gene mutations in newborns with fatal surfactant deficiency. *N. Engl. J. Med.* **350:** 1296–1303.
9. Mulugeta, S., J. M. Gray, K. L. Notarfrancesco, L. W. Gonzales, M. Koval, S. I. Feinstein, P. L. Ballard, A. B. Fisher, and H. Shuman. 2002. Identification of LBM180, a lamellar body limiting membrane protein of alveolar type II cells, as the ABC transporter protein ABCA3. *J. Biol. Chem.* **277:** 22147–22155.
10. Yamano, G., H. Funahashi, O. Kawanami, L. X. Zhao, N. Ban, Y. Uchida, T. Morohoshi, J. Ogawa, S. Shioda, and N. Inagaki. 2001. ABCA3 is a lamellar body membrane protein in human lung alveolar type II cells. *FEBS Lett.* **508:** 221–225.
11. Cheong, N., M. Madesh, L. W. Gonzales, M. Zhao, K. Yu, P. L. Ballard, and H. Shuman. 2006. Functional and trafficking defects in ATP binding cassette A3 mutants associated with respiratory distress syndrome. *J. Biol. Chem.* **281:** 9791–9800.
12. Fitzgerald, M. L., A. J. Mendez, K. J. Moore, L. P. Andersson, H. A. Panjeton, and M. W. Freeman. 2001. ATP-binding cassette transporter A1 contains an NH2-terminal signal anchor sequence that translocates the protein's first hydrophilic domain to the exoplasmic space. *J. Biol. Chem.* **276:** 15137–15145.
13. Yang, Y., and B. Seed. 2003. Site-specific gene targeting in mouse embryonic stem cells with intact bacterial artificial chromosomes. *Nat. Biotechnol.* **21:** 447–451.
14. Ingenito, E. P., R. Mora, M. Cullivan, Y. Marzan, K. Haley, L. Mark, and L. A. Sonna. 2001. Decreased surfactant protein-B expression and surfactant dysfunction in a murine model of acute lung injury. *Am. J. Respir. Cell Mol. Biol.* **25:** 35–44.
15. Devaiah, S. P., M. R. Roth, E. Baughman, M. Li, P. Tamura, R. Jeannotte, R. Welti, and X. Wang. 2006. Quantitative profiling of polar glycerolipid species from organs of wild-type Arabidopsis and a PHOSPHOLIPASE Dalpha1 knockout mutant. *Phytochemistry.* **67:** 1907–1924.
16. Welti, R., W. Li, M. Li, Y. Sang, H. Biesiada, H. E. Zhou, C. B. Rajashekar, T. D. Williams, and X. Wang. 2002. Profiling membrane lipids in plant stress responses. Role of phospholipase D alpha in freezing-induced lipid changes in Arabidopsis. *J. Biol. Chem.* **277:** 31994–32002.
17. Brugger, B., G. Erben, R. Sandhoff, F. T. Wieland, and W. D. Lehmann. 1997. Quantitative analysis of biological membrane lipids at the low picomole level by nano-electrospray ionization tandem mass spectrometry. *Proc. Natl. Acad. Sci. USA.* **94:** 2339–2344.
18. Liebisch, G., B. Lieser, J. Rathenberg, W. Drobnik, and G. Schmitz. 2004. High-throughput quantification of phosphatidylcholine and sphingomyelin by electrospray ionization tandem mass spectrometry coupled with isotope correction algorithm. *Biochim. Biophys. Acta.* **1686:** 108–117.
19. Moore, K. J., V. V. Kunjathoor, S. L. Koehn, J. J. Manning, A. A. Tseng, J. M. Silver, M. McKee, and M. W. Freeman. 2005. Loss of receptor-mediated lipid uptake via scavenger receptor A or CD36 pathways does not ameliorate atherosclerosis in hyperlipidemic mice. *J. Clin. Invest.* **115:** 2192–2201.
20. Carr, T. P., C. J. Andresen, and L. L. Rudel. 1993. Enzymatic determination of triglyceride, free cholesterol, and total cholesterol in tissue lipid extracts. *Clin. Biochem.* **26:** 39–42.

21. Matsumura, Y., N. Ban, K. Ueda, and N. Inagaki. 2006. Characterization and classification of ATP-binding cassette transporter ABCA3 mutants in fatal surfactant deficiency. *J. Biol. Chem.* **281:** 34503–34514.
22. Garmany, T. H., M. A. Moxley, F. V. White, M. Dean, W. M. Hull, J. A. Whitsett, L. M. Nogee, and A. Hamvas. 2006. Surfactant composition and function in patients with ABCA3 mutations. *Pediatr. Res.* **59:** 801–805.
23. Kennedy, M. A., G. C. Barrera, K. Nakamura, A. Baldan, P. Tarr, M. C. Fishbein, J. Frank, O. L. Francone, and P. A. Edwards. 2005. ABCG1 has a critical role in mediating cholesterol efflux to HDL and preventing cellular lipid accumulation. *Cell Metab.* **1:** 121–131.
24. Weng, J., N. L. Mata, S. M. Azarian, R. T. Tzekov, D. G. Birch, and G. H. Travis. 1999. Insights into the function of Rim protein in photoreceptors and etiology of Stargardt's disease from the phenotype in abcr knockout mice. *Cell.* **98:** 13–23.
25. Postle, A. D., L. W. Gonzales, W. Bernhard, G. T. Clark, M. H. Godinez, R. I. Godinez, and P. L. Ballard. 2006. Lipidomics of cellular and secreted phospholipids from differentiated human fetal type II alveolar epithelial cells. *J. Lipid Res.* **47:** 1322–1331.
26. Schlame, M., B. Rustow, D. Kunze, H. Rabe, and G. Reichmann. 1986. Phosphatidylglycerol of rat lung. Intracellular sites of formation de novo and acyl species pattern in mitochondria, microsomes and surfactant. *Biochem. J.* **240:** 247–252.
27. Ridsdale, R., M. Roth-Kleiner, F. D'Ovidio, S. Unger, M. Yi, S. Keshavjee, A. K. Tanswell, and M. Post. 2005. Surfactant palmitoylmyristoylphosphatidylcholine is a marker for alveolar size during disease. *Am. J. Respir. Crit. Care Med.* **172:** 225–232.
28. Beers, M. F., A. Hamvas, M. A. Moxley, L. W. Gonzales, S. H. Guttentag, K. O. Solarin, W. J. Longmore, L. M. Nogee, and P. L. Ballard. 2000. Pulmonary surfactant metabolism in infants lacking surfactant protein B. *Am. J. Respir. Cell Mol. Biol.* **22:** 380–391.
29. Clark, J. C., S. E. Wert, C. J. Bachurski, M. T. Stahlman, B. R. Stripp, T. E. Weaver, and J. A. Whitsett. 1995. Targeted disruption of the surfactant protein B gene disrupts surfactant homeostasis, causing respiratory failure in newborn mice. *Proc. Natl. Acad. Sci. USA.* **92:** 7794–7798.